

Cite this: *Chem. Sci.*, 2017, 8, 7537

Photosensitizer-free visible light-mediated gold-catalysed *cis*-difunctionalization of silyl-substituted alkynes†

Jie-Ren Deng,^{ab} Wing-Cheung Chan,^b Nathanael Chun-Him Lai,^{ab} Bin Yang,^{ab}
Chui-Shan Tsang,^b Ben Chi-Bun Ko,^{‡b} Sharon Lai-Fung Chan^{‡ab}
and Man-Kin Wong^{ib*ab}

A new photosensitizer-free visible light-mediated gold-catalysed *cis*-difunctionalization reaction is developed. The reaction was chemoselective towards silyl-substituted alkynes with excellent regioselectivity and good functional group compatibility, giving a series of silyl-substituted quinolizinium derivatives as products. The newly synthesized fluorescent quinolizinium compounds, named JR-Fluor-1, possessed tunable emission properties and large Stokes shifts. With unique photophysical properties, the fluorophores have been applied in photooxidative amidations as efficient photocatalysts and cellular imaging with switchable subcellular localization properties.

Received 22nd May 2017
Accepted 31st August 2017

DOI: 10.1039/c7sc02294h

rsc.li/chemical-science

Introduction

Over the past years, homogeneous gold catalysis has become a powerful tool for the synthesis of complex organic molecules, particularly in the activation of C–C multiple bonds with gold catalysts acting as strong soft π -Lewis acids.¹ In recent years, instead of accessing hydrofunctionalized products, a promising cross-coupling strategy involving Au(I)/Au(III) catalytic cycles has been developed to afford difunctionalized products.² With a significantly high redox potential of the Au(I)/Au(III) couple, strong oxidants are required to access the oxidation of Au(I) species, while the functional group compatibility could be hampered.^{3a} A complementary approach to overcome this barrier was developed by Glorius³ and Toste⁴ through merging gold catalysis with photoredox catalysis, which promoted oxidation of Au(I) species employing photosensitizers and aryl radicals generated *in situ* under irradiation. This approach inspired the development of diverse organic transformations including difunctionalization of alkenes,^{3b,c,4b} allenes^{5a} and alkynes,^{3e,5b,c} as well as C–C^{3d,4d,5d-f} and C–P^{4c} cross-coupling reactions. Recently, Hashmi and co-workers reported a visible light-mediated gold-catalysed oxyarylation of alkynes^{6a} and an

aryl–aryl coupling reaction^{6b} which could be conducted without addition of photosensitizers.

For alkyne difunctionalization reactions undergoing an anti-nucleophilic addition, *trans*-difunctionalized products are afforded in the majority of the examples.^{3c,e,5c,6a} However, visible light-mediated *cis*-difunctionalization of alkynes still remains largely unexplored.⁷ Inspired by a stereo- and regioselective gold-catalysed hydroamination of internal alkynes reported by Stradiotto *et al.*,⁸ we set out to combine visible light mediated Au(I)/Au(III) catalysis with a plausible *syn* insertion pathway to achieve alkyne *cis*-difunctionalization products (Scheme 1).^{7b,c}

Development of organic fluorescent materials has become an emerging and important research area due to their wide applications in chemistry, biology and materials science.⁹ Compared to the intensive investigations on scaffolds such as fluorescein, BODIPY and, recently, Seoul-Fluor,¹⁰ only a few examples of cationic fluorophores have been reported, although the unique properties of fluorophores containing positive charge have been demonstrated in photocatalysis and cellular imaging.¹¹ Quinoliziniums, cationic aromatic heterocycles bearing a quaternary bridgehead nitrogen, were firstly investigated in alkaloid chemistry and recently employed as efficient DNA intercalators.¹² However, structure photophysical property relationship (SPPR) studies and applications in photocatalysis and cellular imaging of quinolizinium compounds still remain elusive.¹³

Along with our ongoing interest in gold-catalysed organic transformations,¹⁴ herein, we report a new photosensitizer-free visible light-mediated gold-catalysed alkyne *cis*-difunctionalization reaction affording a series of silyl-substituted fluorescent quinolizinium compounds. Spectroscopy experiments and DFT calculations were conducted to study the SPPR of the

^aThe Hong Kong Polytechnic University, Shenzhen Research Institute, Shenzhen, People's Republic of China. E-mail: mankin.wong@polyu.edu.hk

^bState Key Laboratory of Chirosciences, Department of Applied Biology and Chemical Technology, The Hong Kong Polytechnic University, Hung Hum, Hong Kong

† Electronic supplementary information (ESI) available. CCDC 1545248. For ESI and crystallographic data in CIF or other electronic format see DOI: 10.1039/c7sc02294h

‡ Dr Sharon Lai-Fung Chan designed and performed the spectroscopic studies and computational experiments of this research. Dr Ben Chi-Bun Ko designed the cellular imaging experiments.

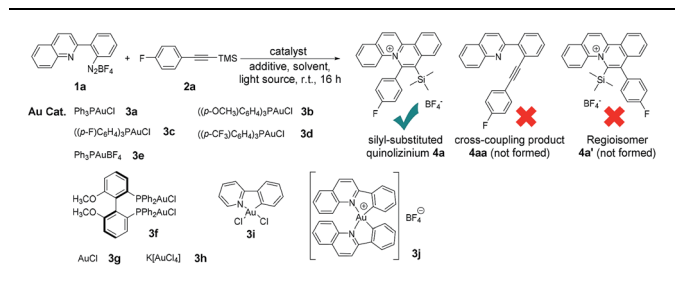
quinolizinium derivatives. Applications of the fluorescent quinolizinium compounds as efficient photocatalysts for photo-oxidative amidation and as fluorescent dyes for live cell imaging have also been conducted.

Results and discussion

We initiated the reaction screening by treatment of quinoline-substituted aryl diazonium **1a** (0.12 mmol, 1.2 equiv.), and (4-fluorophenylethynyl)trimethylsilane **2a** (0.10 mmol, 1 equiv.) with Ph_3PAuCl **3a** (10 mol%) to afford silyl-substituted quinolizinium **4a** in 71% yield (Table 1, entry 1). To our surprise, no cross-coupling product **4aa** (reported by Toste *et al.* using phenyl diazoniums as substrates) was obtained in our experiments.^{4d} Besides, the reaction was exceptionally regioselective giving no regioisomer **4a'**. The gold(i) catalyst **3b** bearing comparatively electron-rich phosphine led to a lower yield of product formation (entry 2), while catalysts **3c–d** bearing electron-poor phosphine gave higher yields of **4a** (entries 3–4). No desired product was obtained when $\text{Ph}_3\text{PAuBF}_4$ **3e** was employed as a catalyst (entry 5). Using gold(i) catalyst **3f** possessing a diphosphine ligand led to product formation in 21% yield (entry 6). Only a trace amount of product was observed when simple AuCl **3g** was used (entry 7). In addition, employing gold(III) catalysts **3h–j** resulted in no product formation (entries 8–10). Without the addition of gold catalyst, no desired product was observed (entry 11), indicating that the gold(i) phosphine chloride catalyst played a crucial role in this transformation. Addition of the transition metal-based photocatalysts $\text{Ru}(\text{bpy})_3\text{Cl}_2$, $\text{Ru}(\text{bpy})_3(\text{BF}_4)_2$ and $\text{Ir}(\text{ppy})_3$ or the organic photocatalyst Rose bengal led to lower yields of the desired product (entries 12–15). A control experiment in the dark gave no product formation (entry 16). These results suggested that this reaction was conducted under photosensitizer-free reaction conditions. Additionally, only a trace amount of product was detected when the reaction was conducted in toluene, dichloromethane or methanol as the solvent (entries 17–19), and a lower yield (35%) of product was afforded when the reaction was carried out in open air (entry 20).

With the optimized reaction conditions, we expanded the scope of this reaction by using various diazoniums (0.60 mmol, 1.2 equiv.) and alkynes (0.50 mmol, 1.0 equiv.) as substrates. Silyl-substituted alkynes **2a–q** bearing ether, alkyl, halogen, aldehyde, carboxylic acid, cyanide, trifluoromethyl, nitro and hetero-aromatics as substituents were well tolerated with the

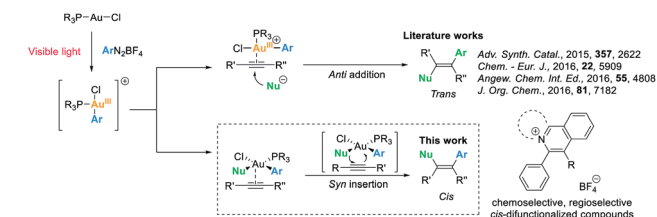
Table 1 Optimization of the reaction conditions and control experiments^a



Entry	Au cat.	Photo cat.	Light	N ₂ /air	Solvent	Yield ^b [%]
1	3a	—	Blue ^c	N ₂	CH ₃ CN	71
2	3b	—	Blue ^c	N ₂	CH ₃ CN	58
3	3c	—	Blue ^c	N ₂	CH ₃ CN	75
4	3d	—	Blue ^c	N ₂	CH ₃ CN	83
5	3e	—	Blue ^c	N ₂	CH ₃ CN	n.d. ^d
6	3f	—	Blue ^c	N ₂	CH ₃ CN	21
7	3g	—	Blue ^c	N ₂	CH ₃ CN	Trace
8	3h	—	Blue ^c	N ₂	CH ₃ CN	n.d. ^d
9	3i	—	Blue ^c	N ₂	CH ₃ CN	n.d. ^d
10	3j	—	Blue ^c	N ₂	CH ₃ CN	n.d. ^d
11	—	—	Blue ^c	N ₂	CH ₃ CN	n.d. ^d
12	3a	$\text{Ru}(\text{bpy})_3\text{Cl}_2$	Blue ^c	N ₂	CH ₃ CN	9
13	3a	$\text{Ru}(\text{bpy})_3(\text{BF}_4)_2$	Blue ^c	N ₂	CH ₃ CN	Trace
14	3a	$\text{Ir}(\text{ppy})_3$	Blue ^c	N ₂	CH ₃ CN	Trace
15	3a	Rose bengal	Blue ^c	N ₂	CH ₃ CN	65
16	3a	—	Dark	N ₂	CH ₃ CN	n.d. ^d
17	3a	—	Blue ^c	N ₂	Toluene	Trace
18	3a	—	Blue ^c	N ₂	CH ₂ Cl ₂	Trace
19	3a	—	Blue ^c	N ₂	CH ₃ OH	Trace
20	3a	—	Blue ^c	Air	CH ₃ CN	35

^a Reaction conditions: treatment of **1a** (0.12 mmol), **2a** (0.10 mmol) and gold catalyst **3a–j** (10 mol%) with or without photocatalyst (5 mol%) in 5 mL of solvent under N₂ at room temperature for 16 h. ^b Yield of **4a** was determined by ¹⁹F-NMR using fluorobenzene as the internal standard. ^c Blue LEDs ($\lambda_{\text{max}} = 469 \text{ nm}$) were employed as a light source. ^d n.d.: product formation could not be detected.

reactions giving quinolizinium products **4a–q** in 31–69% yield. Increasing the steric bulkiness using *ortho*-disubstituted phenylethynylsilane **2r** gave a trace amount of product. Using a triethylsilyl group gave quinolizinium **4u** in slightly lower yield (45%). Further increasing the bulkiness employing *tert*-butyldiphenylsilyl-substituted alkyne **2t** gave no product **4v**. Interestingly, employing terminal alkyne phenylacetylene **2u**, cyclohexylacetylene **2v** or internal alkyne 1,2-diphenylethyne **2w**, 1-phenyl-1-propyne **2x** or 1-phenyl-1-butyne **2y** gave no desired product **7a–e**, suggesting that the reaction was chemoselective towards silyl-substituted alkynes. To support our hypothesis, alkyne **2z** bearing diphenylethynyl and trimethylsilylethynyl groups was used, and only the trimethylsilylethynyl *cis*-difunctionalized product **4w** was obtained in 46% yield, which convinced us of the chemoselectivity of this gold-catalysed transformation. Further expansion of the scope employing diazoniums **1b–d** bearing different structure skeletons and heterocycles gave the desired products **5a–c** and **6a** in up to 60% yield. These results indicated that the reaction was



Scheme 1 Literature works and our strategy for visible light-mediated gold-catalysed alkyne *cis*-difunctionalization.



Table 2 Expansion of the substrate scope^{a,b}

4a (65%)	4b (69%)	4c (66%)	4d (68%)	4e (66%)
4f (58%)	4g (31%)	4h (53%)	4i (56%)	4j (65%)
4k (45%)	4l (58%)	4m (68%)	4n (65%)	4o (62%)
4p (63%)	4q (61%)	4r (trace)	4s (63%)	4t (65%)
4u (45%)	5a (34%)	5b (50%)	5c (37%)	6a (60%)
4v (not formed)	7a (not formed)	7b (not formed)	7c (not formed)	7d (not formed)
7e (not formed)	7f (not formed)	7g (not formed)	7h (not formed)	7i (not formed)

^a Reaction conditions: treatment of **1a-d** (0.60 mmol), **2a-z** (0.50 mmol) and **3a** (10 mol%) in 5 mL of CH₃CN under irradiation (blue LEDs) and N₂ at room temperature for 16 h. ^b Isolated yield.

very compatible with various diazoniums and highly selective towards silyl-substituted alkynes (Table 2).

To provide insight into this visible light-mediated gold-catalysed *cis*-difunctionalization reaction, stoichiometric reactions were set up by treatment of aryl diazonium **1a** (0.10 mmol) with Ph₃PAuCl **3a** (0.10 mmol) under irradiation for 0 to 240 min. ¹H-NMR monitoring revealed that aryl diazonium **1a** was consumed and new signals appeared gradually from 0 to 60 min, suggesting the formation of plausible intermediates (Fig. 1a). Irradiation for a longer time gave a slight decomposition of the plausible intermediates. These results were consistent with those observed by ³¹P-NMR analysis, which indicated the gradual appearance of new signals at 31.0, 44.2 and 45.3 ppm (Fig. 1b). The reaction mixtures were further

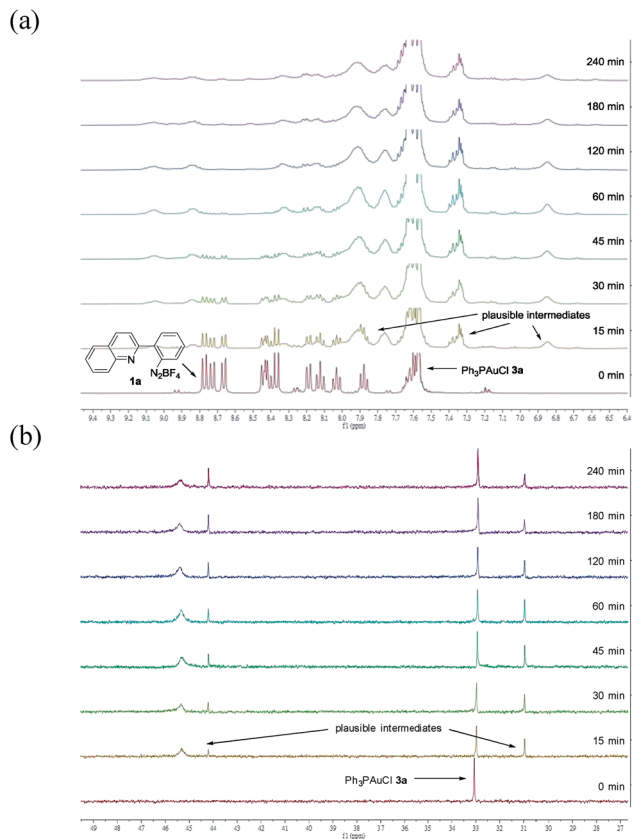


Fig. 1 (a) ¹H-NMR studies on reaction mixtures X₀–240 min in CD₃CN; (b) ³¹P-NMR studies on reaction mixtures X₀–240 min in CD₃CN.

treated with silyl-substituted alkyne **2a** (1.5 equiv.) for 60 min in the dark, resulting in the disappearance of the newly observed signals after irradiation and concomitant formation of the signals of the quinolinizinium product **4a** (Fig. S3a and b in the ESI†). The yield of the product formed was monitored by ¹⁹F-NMR analysis through the addition of fluorobenzene as the internal standard (Fig. S3c in the ESI†). In addition, regeneration of Ph₃PAuCl **3a** could be recovered as a precipitate from the reaction mixtures.

Due to difficulties in the isolation of the reaction intermediates, we sought to investigate the plausible Au(III) species through ESI-MS analysis by treatment of aryl diazonium **1a** (0.12 mmol) with Ph₃PAuCl **3a** (0.10 mmol) under irradiation for 1 h. The experimental results indicated that rather than the formation of **A** (*m/z* = 204.0792) by the displacement of N₂ of **1a** in ESI-MS analysis, plausible Au(III) intermediates **B** (*m/z* = 698.1014) and **B'** (*m/z* = 960.1910) were found (Fig. 2a). Further treatment of the afforded reaction mixture **Y** with silyl-substituted alkyne **2a** (1.5 equiv.) in the dark for 1 h afforded reaction mixture **Y'**. ESI-MS analysis of reaction mixture **Y'** revealed that no signal for **B** or **B'** was observed, and the signal of the quinolinizinium product **4a** appeared, suggesting that both **B** and **B'** were consumed and reacted with **2a** to form the quinolinizinium product **4a** (Fig. 2b). For a detailed understanding of the plausible Au(III) intermediates **B** and **B'**, ESI-MS/MS analysis of species **B** (precursor ion *m/z* = 698) and **B'** (precursor ion *m/z* =



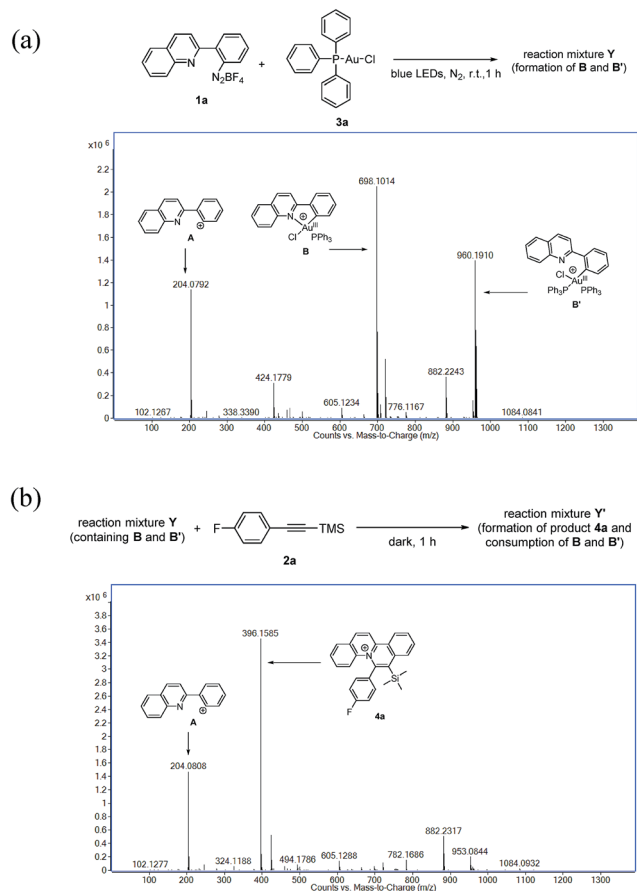


Fig. 2 (a) ESI-MS analysis of the reaction mixture Y; (b) ESI-MS analysis of the reaction mixture Y'.

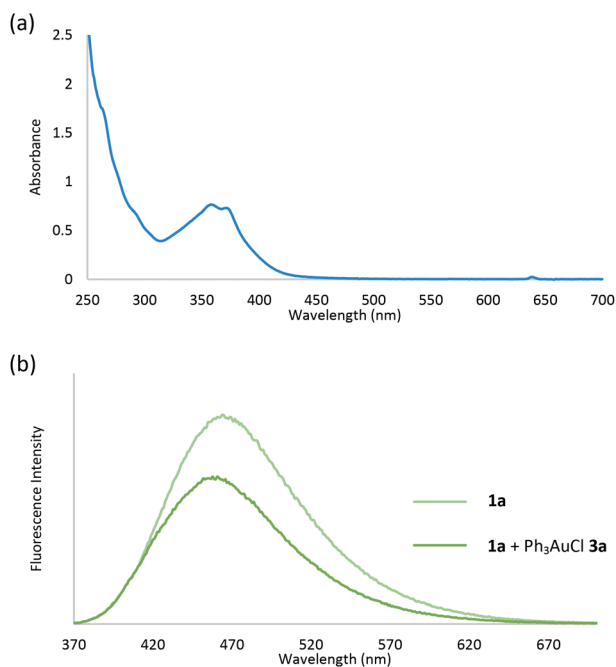
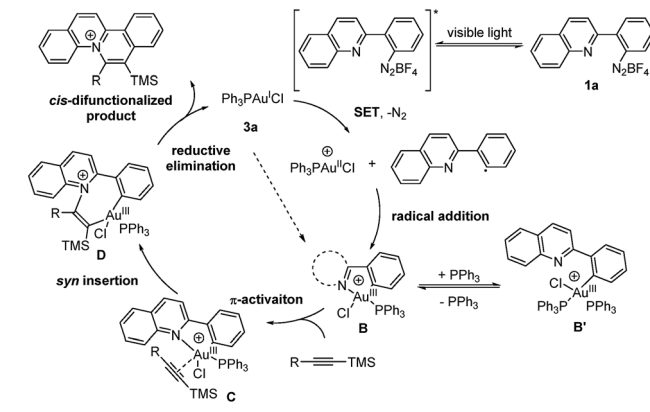


Fig. 3 (a) UV/Vis absorption spectrum of aryl diazonium **1a**; (b) fluorescence quenching of aryl diazonium **1a** with Ph_3PAuCl **3a**.



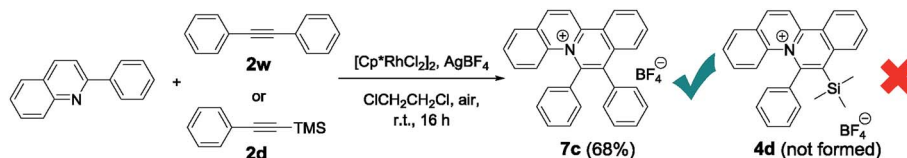
Scheme 2 Proposed reaction mechanism.

910) was conducted. Product phosphonium ions **B-I** ($m/z = 459.0483$) and Au(I) species **B-II** ($m/z = 466.1634$) were found in the MS/MS analysis of species **B** (Fig. S4a in the ESI†). Formation of **B-I** was assumed to be ascribed to the reductive elimination of the Au(III) species **B**, which was previously reported as a feasible deactivation pathway of phosphine-supported aryl Au(III) complexes.¹⁵ In MS/MS analysis of species **B'**, product ions of **B** ($m/z = 698.0994$), **B-I** ($m/z = 466.1672$) and **B-II** ($m/z = 459.0518$) were found (Fig. S3b in the ESI†). Results suggested that species **B'** was composed of Au(III) species **B** and triphenylphosphine and presumably formed by possible transmetallation.¹⁶ A control experiment under the same reaction conditions without irradiation led to no formation of the Au(III) species **B**, **B'** or product **4a**, suggesting that a light source was necessary for promotion of the Au(I)/Au(III) transformation in this reaction.

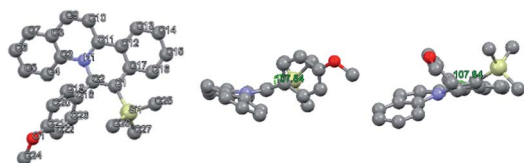
To study the photosensitizer-free reaction conditions, we measured the UV/Vis absorption properties of aryl diazonium **1a** and Ph_3PAuCl **3a**. Spectroscopic analysis revealed that no absorption peak of Ph_3PAuCl **3a** was observed at $\lambda_{\text{abs}} > 395$ nm (Fig. S6 in the ESI†), indicating that Ph_3PAuCl **3a** might not be directly excited by the light source in this reaction which was consistent with literature work indicating that the photosensitizer was necessary to initiate the reaction.^{3–5} On the contrary, a tail of the lowest energy absorption peak of aryl diazonium **1a** was found at $\lambda_{\text{abs}} > 395$ nm (Fig. 3a), suggesting that aryl diazoniums could be firstly excited to initiate the reaction.¹⁷ To further support our hypothesis, we measured the difference of the fluorescence intensity before and after mixing Ph_3PAuCl **3a** (1 equiv.) with **1a**. Spectroscopic analysis indicated that the fluorescence of **1a** could be quenched ($I_{\text{q}}/I_0 = 0.68$) after the addition of Ph_3PAuCl **3a**, providing strong evidence for electron transfer from Ph_3PAuCl **3a** to aryl diazonium **1a** under irradiation (Fig. 3b). In addition, the estimated excited state reduction potential (E_{red}^*) of aryl diazonium **1a** was 3.28 V, which was much higher than the redox potential of the Au(I)/Au(III) couple ($E_0 = 1.41$ V),¹⁸ indicating that Ph_3PAuCl **3a** could be oxidized by the aryl diazonium **1a** in the first step of the reaction.

Based on the aforementioned experimental results, a reaction mechanism is proposed as shown (Scheme 2). Under





Scheme 3 Rhodium-catalysed synthesis of quinolizinium compounds.

Fig. 4 X-ray crystal structure of **4b** (front view, left view and vertical view).

irradiation, the aryl diazonium compound is firstly excited and subsequently reduced by single electron transfer from Au(I) catalyst **3a** to form an aryl radical with the generation of a Au(II) species. The Au(II) species further recombines with the aryl radical to give Au(III) intermediate **B**. The oxidation and addition on Au(I) catalyst **3a** to form Au(III) intermediate **B** is also possibly a concerted reaction pathway rather than a two-step process.^{6a} The reaction quantum yield was found to be 0.91 (less than 1), suggesting that the radical chain process was not prominent in this transformation. Then, silyl-substituted alkyne is activated

by Au(III) intermediate **B** through π -activation to give species **C**. After that, the Au–N bond is regioselectively inserted by the π -activated alkyne to form *cis* vinyl gold species **D**. Then, reductive elimination provides a quinolizinium compound as the *cis*-difunctionalized product and regenerates the Au(I) catalyst **3a**.

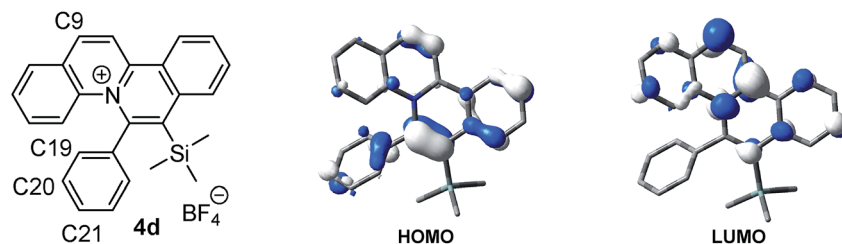
Pioneered by Cheng and co-workers,¹⁹ rhodium-catalysed C–H bond activation followed by annulation has been used as a powerful tool for the synthesis of disubstituted quinolizinium compounds. We sought to compare the newly developed approach of gold-catalysed *cis*-difunctionalization with rhodium catalysis. An optimized reaction employing 2-phenylquinoline (0.1 mmol, 1 equiv.) with internal alkyne 1,2-diphenylethyne **2w** (0.1 mmol, 1 equiv.), [Cp*RhCl₂]₂ (5 mol%) and AgBF₄ (0.1 mmol, 1 equiv.) in 1,2-dichloroethane under open air at room temperature for 16 h afforded diphenyl-substituted quinolizinium **7c** in 68% yield. However, when 1-phenyl-2-trimethylsilylacetylene **2d** was employed as a substrate, no desired product **4d** was formed. To our knowledge, the present photosensitizer-free visible light-mediated gold-catalysed

Table 3 Photophysical properties of quinolizinium compounds **4a–q**, **s–u**, **w** and **5a–c**^a

Cpd.	Absorption maximum λ_{abs} (nm) (ϵ (10 ⁴ dm ³ mol ^{−1} cm ^{−1}))	Emission maximum λ_{em} (nm)	Stokes shift (cm ^{−1})	Quantum yield Φ_{F} ^b
4a	423 (1.39)	495	3439	0.49
4b	430 (1.14)	569	5681	0.17
4c	428 (1.10)	507	3640	0.44
4d	423 (1.45)	491	3275	0.44
4e	424 (1.62)	494	3342	0.37
4f	422 (0.95)	493	3413	0.16
4g	424 (1.00)	493	3301	0.03
4h	423 (1.06)	480	2807	0.28
4i	417 (0.75)	484	3320	0.44
4j	420 (1.30)	479	2933	0.28
4k	420 (1.17)	479	2933	0.34
4l	419 (1.23)	476	2858	0.24
4m	423 (1.45)	506	3878	0.18
4n	424 (1.68)	508	3900	0.16
4o	428 (1.43)	547	5363	0.02
4p	421 (1.50)	511	4183	0.11
4q	423 (1.80)	511	4071	0.16
4s	446 (0.79)	640	6797	0.01
4t	446 (1.05)	557	4468	0.08
4u	424 (1.42)	494	3342	0.41
4w	427 (1.05)	555	5401	0.07
5a	397 (1.74)	495	4987	0.02
5b	405 (1.23)	504	4850	0.30
5c	401 (1.09)	450	2840	0.59

^a Absorption and emission properties were measured in CH₂Cl₂ at a concentration of 1×10^{-5} M. ^b Quantum yields were measured using fluorescein ($\Phi_{\text{F}} = 0.95$ in 0.1 N NaOH buffer) as a standard.



Fig. 5 HOMO and LUMO diagrams of **4d**.Table 4 Photooxidative amidation using quinolizinium compounds as photocatalysts^a

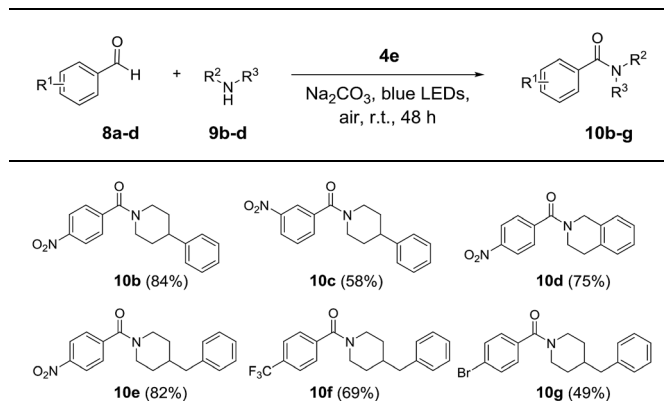
Entry	Photo cat.	E_{red}^* (V)	Time (h)	Yield ^b [%]
1	4a	1.99	16	53
2	4b	1.97	16	50
3	4e	2.21	16	61
4	4f	2.22	16	59
5	4j	2.24	16	52
6	4p	2.07	16	53
7	Eosin Y	1.23 ^c	16	48
8	Fluorescein	1.25 ^c	16	47
9	Rose Bengal	1.18 ^c	16	32
10	[Acr ⁺ -Mes](BF ₄)	2.08 ^c	16	44
11	4e	2.21	48	86
12 ^d	4e	2.21	48	71 ^e

^a Reaction conditions: treatment of **8a** (0.1 mmol, 1 equiv.), **9a** (0.2 mmol, 2 equiv.), Na₂CO₃ (0.2 mmol, 2 equiv.) and photocatalyst (5 mol%) in 5 mL of CH₃CN under blue LEDs and air at room temperature. ^b Yield was determined by ¹H-NMR using 1,3,5-trimethoxybenzene as the internal standard. ^c E_{red}^* refers to ref. 9a and literature cited there. ^d Reaction was performed by treatment of **8a** (1 mmol, 1 equiv.), **9a** (2 mmol, 2 equiv.), Na₂CO₃ (2 mmol, 2 equiv.) and photocatalyst (5 mol%) in 5 mL of CH₃CN under blue LEDs and air at room temperature. ^e Isolated yield.

alkyne *cis*-difunctionalization is the first example of a highly regioselective synthesis of silyl-substituted quinolizinium compounds (Scheme 3).

X-ray crystal structure analysis revealed a twisted conformation of quinolizinium **4b**, with a torsion angle of 107.84° (C1–C2–C18–C19), suggesting that the molecule could be divided into two parts: a slightly distorted planar quinolizinium moiety and a phenyl moiety. This twisted structure suggested that the two moieties should be weakly coupled conjugatively (Fig. 4).

After synthesis of the new silyl-substituted quinolizinium compounds, we moved on to study their absorption and emission properties (Table 3). Interestingly, these compounds possessed the lowest energy absorption maxima at $\lambda_{\text{abs}} > 395$ nm, full color tunable emission properties ($\lambda_{\text{em}} = 450$ to 640 nm) in the visible light region and large Stokes shifts (up to

Table 5 Photooxidative amidation of aldehydes with secondary amines^{a,b}

^a Reaction conditions: treatment of **8a-d** (0.1 mmol, 1 equiv.), **9b-d** (0.2 mmol, 2 equiv.), Na₂CO₃ (0.2 mmol, 2 equiv.) and photocatalyst **4e** (5 mol%) in 5 mL of CH₃CN under blue LEDs and air at room temperature for 48 h. ^b Isolated yield.

6797 cm^{−1}) with quantum yields up to 0.59. Incorporation of electron-donating groups at the *para*-position of the phenyl moiety or introduction of π -excessive heteroaromatics resulted in bathochromic shifts of the emission properties. Further bathochromic shifts were observed by the introduction of an electron-withdrawing ester group on the quinolizinium moiety. Substituents bearing heavy atoms (Cl, Br, I) led to lower quantum yields. A positive solvatochromism was found in compound **4b**, which indicated an increase of dipole moment of the excited state compared to its ground state (Fig. S8 in the ESI†). An unexpectedly low quantum yield of **5a** (0.02) bearing a dimethylamine substituent was observed, in which the fluorescence was proposed to be quenched by the amine group *via* intramolecular photo-induced electron transfer (PET). Cyclic voltammetry (CV) experiments indicated a quasireversible oxidation couple at +1.08 V (vs. SCE) of **5a** which originated from the presence of the amine group and no similar peak was found in **5c** (ESI†). Protonation of the amine group by measuring the emission in HCl/NaOH buffer (pH changing from 7 to 1) gave a ≥ 100 fold enhancement of the emission intensity at a shorter wavelength ($\lambda_{\text{em}} = 436$ nm) which supported our hypothesis (Fig. S9 in the ESI†).

For a detailed investigation of the SPPR of the quinolizinium compounds, compound **4d** was subjected to TDDFT



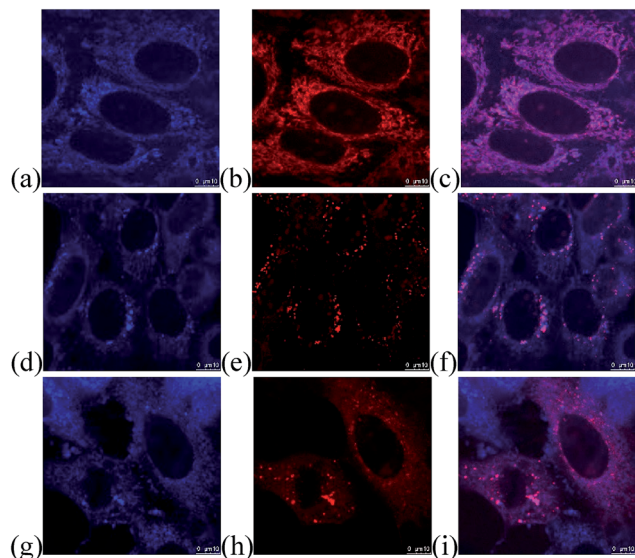


Fig. 6 Confocal fluorescence microscopic images of HeLa cells. (a) Sub-cellular localization of **5c**; (b) subcellular localization of MitoTracker® red; (c) merged images of (a) and (b); (d) subcellular localization of **4l**; (e) subcellular localization of LysoTracker® deep red; (f) merged images of (d) and (e); (g) subcellular localization of **4l**; (h) subcellular localization of mRFP-Rab7; (i) merged images of (g) and (h).

calculations. Results reveal that the lowest energy absorption band at 435 nm is originated from HOMO \rightarrow LUMO transitions. The HOMO is composed of a π orbital of the quinolizinium and phenyl ring whereas the LUMO is composed of a π^* orbital of the quinolizinium ring. The low energy absorption band can be assigned as an admixture of $\pi \rightarrow \pi^*$ transitions within the quinolizinium ring and $\pi \rightarrow \pi^*$ transitions from the phenyl to quinolizinium ring. Hence, bathochromic shifts were observed by the introduction of an ester group at C9 (LUMO was dominant) and the introduction of electron-donating groups at C21 (HOMO was partially dominant) (Fig. 5).

In line with our interest in amide synthesis,²⁰ we envisioned that the newly developed quinolizinium fluorophores could be utilized as photocatalysts for photooxidative amidation of aldehydes and secondary amines. We first investigated the catalytic activities by treatment of 4-nitrobenzaldehyde **8a** (0.1 mmol, 1 equiv.), piperidine **9a** (0.2 mmol, 2 equiv.), Na_2CO_3 (0.2 mmol, 2 equiv.) and selected photocatalysts (5 mol%) in CH_3CN under irradiation (blue LEDs) and air for 16 h. Interestingly, the catalytic activities of quinoliziniums were comparable or even better than the currently used photocatalysts (Table 4). The reaction was optimized using **4e** as a photocatalyst to afford amide **10a** in 86% yield after 48 h. Expansion of the scope employing different aldehydes and secondary amines gave amides **10b–g** in up to 84% yield (Table 5). Further investigations revealed that the quinolizinium compounds possessed tunable and high excited state reduction potentials ($E_{\text{red}}^* = 1.97$ to 2.23 V), which were comparable to the well-known photocatalyst 9-mesityl-10-methylacridinium [$\text{Acr}^+ \text{Mes}$](BF_4) developed by Fukuzumi.²¹ To our knowledge, this is

the first example of employing quinoliziniums as photocatalysts for visible light-mediated photoredox catalysis.

The feasibility in cellular imaging was demonstrated by incubation of HeLa cells with 2 μM of the fluorescent quinolizinium compounds **4a–b**, **d**, **f**, **h**, **l–o**, **s–t**, **w** and **5c**, respectively (Experimental details in the ESI†). Confocal fluorescence microscopic images revealed that the quinoliziniums were selectively localized in cytoplasm with no transportation into the nucleus, which was different from the known examples of quinoliziniums.²² Compound **5c** and **4l** were chosen for colocalization studies to track the subcellular localization. Compound **5c** was specifically localized in the mitochondria (Fig. 6a–c), which could be attributed to the presence of the positively charged quinolizinium skeleton, directing it towards the mitochondria membrane with -180 mV potential. Interestingly, apart from localization in the mitochondria, compound **4l** bearing a nitro substituent localized mainly in the lysosome and partially in late the endosome (Fig. 6d–i). The subcellular localization of the quinoliziniums could be switched by simply modifying the substituents, and these compounds would be amenable for the design of specific molecular probes for individual organelle imaging.

Conclusions

In summary, we have developed the first photosensitizer-free visible light-mediated gold-catalysed *cis*-difunctionalization reaction with high chemoselectivity and excellent regioselectivity for modular synthesis of a series of silyl-substituted quinolizinium compounds. Control experiments as well as a combination of NMR, ESI-MS and spectroscopic analysis indicate a plausible visible light-mediated $\text{Au}(\text{I})/\text{Au}(\text{III})$ catalytic transformation involving a regioselective *syn* insertion of silyl-substituted alkynes. Additionally, we have studied applications of the newly synthesized silyl-substituted quinolizinium compounds in photooxidative amidation and cellular imaging. The efficient modular synthesis and unique photophysical properties of the quinolizinium compounds will open up a new direction in gold catalysis, photoredox catalysis and molecular imaging.

Conflicts of interest

M.-K. Wong, J.-R. Deng and N. C.-H. Lai applied patents on quinolizinium compounds **4a–q**, **s–u**, **w** and **5a–c**.

Acknowledgements

We are grateful for the financial support of the National Natural Science Foundation of China (21272198), Hong Kong Research Grants Council (PolyU 153031/14P, 153001/17P, X-ray diffractometer-PolyU11/CRF/13E), State Key Laboratory of Chirosciences and Department of Applied Biology and Chemical Technology. We thank Prof. K.-Y. Wong for facilitating the project by providing access to Bioanalytical Systems (BAS) for cyclic voltammetry experiments and Prof. Z. Zhou and Dr W. T.-K. Chan for X-ray crystallographic analysis.



Notes and references

- 1 (a) A. S. K. Hashmi and G. J. Hutchings, *Angew. Chem., Int. Ed.*, 2006, **45**, 7896; (b) A. S. K. Hashmi, *Chem. Rev.*, 2007, **107**, 3180; (c) Z. Li, C. Brouwer and C. He, *Chem. Rev.*, 2008, **108**, 3239; (d) A. Arcadi, *Chem. Rev.*, 2008, **108**, 3266; (e) E. Jiménez-Núñez and A. M. Echavarren, *Chem. Rev.*, 2008, **108**, 3326; (f) D. J. Gorin, B. D. Sherry and F. D. Toste, *Chem. Rev.*, 2008, **108**, 3351; (g) N. Krause and C. Winter, *Chem. Rev.*, 2011, **111**, 1994; (h) H.-S. Yeom and S. Shin, *Acc. Chem. Res.*, 2014, **47**, 966; (i) Z. Zheng, Z. Wang, Y. Wang and L. Zhang, *Chem. Soc. Rev.*, 2016, **45**, 4448; (j) A. M. Asiri and A. S. K. Hashmi, *Chem. Soc. Rev.*, 2016, **45**, 4471; (k) W. Zi and F. D. Toste, *Chem. Soc. Rev.*, 2016, **45**, 4567.
- 2 (a) M. N. Hopkinson, A. D. Gee and V. Gouverneur, *Chem.–Eur. J.*, 2011, **17**, 8248; (b) H. A. Wegner and M. Auzias, *Angew. Chem., Int. Ed.*, 2011, **50**, 8236.
- 3 (a) M. N. Hopkinson, A. Tlahuext-Aca and F. Glorius, *Acc. Chem. Res.*, 2016, **49**, 2261; (b) B. Sahoo, M. N. Hopkinson and F. Glorius, *J. Am. Chem. Soc.*, 2013, **135**, 5505; (c) M. N. Hopkinson, B. Sahoo and F. Glorius, *Adv. Synth. Catal.*, 2014, **356**, 2794; (d) A. Tlahuext-Aca, M. N. Hopkinson, B. Sahoo and F. Glorius, *Chem. Sci.*, 2016, **7**, 89; (e) A. Tlahuext-Aca, M. N. Hopkinson, R. A. Garza-Sanchez and F. Glorius, *Chem.–Eur. J.*, 2016, **22**, 5909.
- 4 (a) M. D. Levin, S. Kim and F. D. Toste, *ACS Cent. Sci.*, 2016, **2**, 293; (b) X.-Z. Shu, M. Zhang, Y. He, H. Frei and F. D. Toste, *J. Am. Chem. Soc.*, 2014, **136**, 5844; (c) Y. He, H. Wu and F. D. Toste, *Chem. Sci.*, 2015, **6**, 1194; (d) S. Kim, J. Rojas-Martinab and F. D. Toste, *Chem. Sci.*, 2016, **7**, 85.
- 5 (a) D. V. Patil, H. Yun and S. Shin, *Adv. Synth. Catal.*, 2015, **357**, 2622; (b) J. Um, H. Yun and S. Shin, *Org. Lett.*, 2016, **18**, 484; (c) Z. Xia, O. Khaled, V. Mouriès-Mansuy, C. Ollivier and L. Fensterbank, *J. Org. Chem.*, 2016, **81**, 7182; (d) T. Cornilleau, P. Hermange and E. Fouquet, *Chem. Commun.*, 2016, **52**, 10040; (e) V. Gauchot and A.-L. Lee, *Chem. Commun.*, 2016, **52**, 10163; (f) V. Gauchot, D. R. Sutherland and A.-L. Lee, *Chem. Sci.*, 2017, **8**, 2885.
- 6 (a) L. Huang, M. Rudolph, F. Rominger and A. S. K. Hashmi, *Angew. Chem., Int. Ed.*, 2016, **55**, 4808; (b) S. Witzel, J. Xie, M. Rudolph and A. S. K. Hashmi, *Adv. Synth. Catal.*, 2017, **359**, 1522.
- 7 (a) M. Joost, A. Amgoune and D. Bourissou, *Angew. Chem., Int. Ed.*, 2015, **54**, 15022; (b) F. Rekhroukh, R. Brousses, A. Amgoune and D. Bourissou, *Angew. Chem., Int. Ed.*, 2015, **54**, 1266; (c) F. Rekhroukh, C. Blons, L. Estévez, S. Mallet-Ladeira, K. Miqueu, A. Amgoune and D. Bourissou, *Chem. Sci.*, 2017, **8**, 4539; (d) C. Gryparis, M. Kidonakis and M. Stratakis, *Org. Lett.*, 2013, **15**, 6038; (e) C. Gryparis and M. Stratakis, *Org. Lett.*, 2014, **16**, 1430.
- 8 K. D. Hesp and M. Stradiotto, *J. Am. Chem. Soc.*, 2010, **132**, 18026.
- 9 (a) N. A. Romero and D. A. Nicewicz, *Chem. Rev.*, 2016, **116**, 10075; (b) X. Li, X. Gao, W. Shi and H. Ma, *Chem. Rev.*, 2014, **114**, 590; (c) H. Uoyama, K. Goushi, K. Shizu, H. Nomura and C. Adachi, *Nature*, 2012, **492**, 234; (d) G. J. Hedley, A. Ruseckas and I. D. W. Samuel, *Chem. Rev.*, 2017, **117**, 796.
- 10 (a) H. Kobayashi, M. Ogawa, R. Alford, P. L. Choyke and Y. Urano, *Chem. Rev.*, 2010, **110**, 2620; (b) A. Loudet and K. Burgess, *Chem. Rev.*, 2007, **107**, 4891; (c) E. Kim, Y. Lee, S. Lee and S. B. Park, *Acc. Chem. Res.*, 2015, **48**, 538.
- 11 (a) Z. Xu and L. Xu, *Chem. Commun.*, 2016, **52**, 1094; (b) W. Xu, Z. Zeng, J. H. Jiang, Y. T. Chang and L. Yuan, *Angew. Chem., Int. Ed.*, 2016, **55**, 13658.
- 12 (a) G. Anton and I. Heiko, *Synlett*, 2016, **27**, 1775; (b) D. Sucunza, A. M. Cuadro, J. Alvarez-Builla and J. J. Vaquero, *J. Org. Chem.*, 2016, **81**, 10126; (c) A. Granzhan, H. Ihmels and G. Viola, *J. Am. Chem. Soc.*, 2007, **129**, 1254.
- 13 A. Barbafina, A. M. Melia, L. Latterini, G. G. Aloisi and F. Elisei, *J. Phys. Chem. A*, 2009, **113**, 14514.
- 14 (a) V. K.-Y. Lo, Y. Liu, M.-K. Wong and C.-M. Che, *Org. Lett.*, 2006, **8**, 1529; (b) H.-M. Ko, K. K.-Y. Kung, J.-F. Cui and M.-K. Wong, *Chem. Commun.*, 2013, **49**, 8869; (c) J.-F. Cui, H.-M. Ko, K.-P. Shing, J.-R. Deng, N. C.-H. Lai and M.-K. Wong, *Angew. Chem., Int. Ed.*, 2017, **56**, 3074.
- 15 H. Kawai, W. J. Wolf, A. G. DiPasquale, M. S. Winston and F. D. Toste, *J. Am. Chem. Soc.*, 2016, **138**, 587.
- 16 W. J. Wolf, M. S. Winston and F. D. Toste, *Nat. Chem.*, 2014, **6**, 159.
- 17 M. S. Winston, W. J. Wolf and F. D. Toste, *J. Am. Chem. Soc.*, 2014, **136**, 7777.
- 18 S. G. Bratsch, *J. Phys. Chem. Ref. Data*, 1989, **18**, 1.
- 19 (a) C.-Z. Luo, P. Gandeepan and C.-H. Cheng, *Chem. Commun.*, 2013, **49**, 8528; (b) C.-Z. Luo, P. Gandeepan, J. Jayakumar, K. Parthasarathy, Y.-W. Chang and C.-H. Cheng, *Chem.–Eur. J.*, 2013, **19**, 14181; (c) C.-Z. Luo, P. Gandeepan, Y.-C. Wu, C.-H. Tsai and C.-H. Cheng, *ACS Catal.*, 2015, **5**, 4837.
- 20 (a) W.-K. Chan, C.-M. Ho, M.-K. Wong and C.-M. Che, *J. Am. Chem. Soc.*, 2006, **128**, 14796; (b) A. O.-Y. Chan, C.-M. Ho, H.-C. Chong, Y.-C. Leung, J.-S. Huang, M.-K. Wong and C.-M. Che, *J. Am. Chem. Soc.*, 2012, **134**, 2589; (c) G.-L. Li, K. K.-Y. Kung and M.-K. Wong, *Chem. Commun.*, 2012, **48**, 4112; (d) F. K.-C. Leung, J.-F. Cui, T.-W. Hui, K. K.-Y. Kung and M.-K. Wong, *Asian J. Org. Chem.*, 2015, **4**, 533.
- 21 S. Fukuzumi, H. Kotani, K. Ohkubo, S. Ogo, N. V. Tkachenko and H. Lemmetyinen, *J. Am. Chem. Soc.*, 2004, **126**, 1600.
- 22 (a) R. Bortolozzi, H. Ihmels, L. Thomas, M. Tian and G. Viola, *Chem.–Eur. J.*, 2013, **19**, 8736; (b) A. C. Shaikh, D. S. Ranade, P. R. Rajamohanan, P. P. Kulkarni and N. T. Patil, *Angew. Chem., Int. Ed.*, 2017, **56**, 757.

